Materials Transactions, Vol. 49, No. 3 (2008) pp. 554 to 558

Tensile Properties of Forged Mg-Al-Zn-Ca Alloy

Masataka Hakamada[1], Akira Watazu[1], Naobumi Saito[1] and Hajime Iwasaki[2]

[1]*Materials Research Institute for Sustainable Development, National Institute of Advanced Industrial Science and Technology, Nagoya 463-8560, Japan*
[2]*The Materials Process Technology Center, Tokyo 105-0011, Japan*

Continuously-casted Mg-9Al-1Zn-1Ca (in mass%) alloy (Mg-Ca alloy) and Mg-9Al-1Zn alloys (Ca-free Mg alloy) were forged at 573 K and their mechanical properties were investigated by tension tests at ambient temperature and 573 K. The forged Mg-Ca alloy showed higher 0.2% proof stress than the forged Ca-free Mg alloy. The high strength for the Mg-Ca alloy was attributed not only to grain refinement by hot forging, but also to the strengthening mechanisms arising from the difference in thermal expansion and geometrical incompatibility between Mg matrix and second phase. The Ca addition decreased the elongation to failure; however, the decrease was reduced for the forged specimens, compared to the unforged specimen. This results from segmentation of the second phases by the hot forging. Also, the forged Mg-Ca alloy showed a large elongation of 284% at 573 K. [doi:10.2320/matertrans.MRA2007261]

(Received October 30, 2007; Accepted December 25, 2007; Published February 25, 2008)

Keywords: *magnesium-calcium alloy, tension test, mechanical properties, cavitation, superplasticity, grain refinement*

1. Introduction

Mg alloys are currently the lightest alloys used as structural metals. Mg products have been applied for structural uses such as automobile parts and electric appliance cases.[1)] For more extensive application of Mg alloys, it is desirable to develop high performance Mg alloys showing high strength, high workability and so on. It has been reported that Mg alloys containing Ca show high creep resistance and elevated temperature strength.[2–6)] Besides, Ca is effective as fire retardant.[7)] For commercial applications, Ca is desirable as an additional element to Mg because of its lower cost, compared with rare earth elements.

In Mg-Al-Ca alloys, insoluble second phases such as Al_2Ca and Mg_2Ca are formed. Such second phases serve as nucleation sites for dynamic recrystallization during hot deformation, and fine-grained microstructure is anticipated in the Mg-Al-Ca alloys. Therefore, Ca addition may improve mechanical properties of the Mg alloys at not only elevated temperature, but also ambient temperature, due to the grain refinement. On the other hand, Ca addition may be harmful because crack or void formation is enhanced by the second phases.[8)] Until now, there are few studies on grain refinement mechanical properties of the Mg-Al-Ca alloys after the grain refinement.[9–12)] In the present paper, Mg-Al-Zn-Ca and Mg-Al-Zn alloy are forged at 573 K and the mechanical properties of the forged and unforged alloys are investigated by tension tests at ambient temperature and 573 K. Based on the results, effects of Ca addition on the mechanical properties are discussed.

2. Experimental Procedure

The Mg-9Al-1Zn-1Ca (in mass%) alloy (denoted as 'Mg-Ca alloy') billet with the diameter of 155 mm, prepared by continuous casting method, was purchased from Sankyo Tateyama Aluminium, Inc. (Toyama, Japan). For comparison, the 155-mm-diameter billet of a Mg-9Al-1Zn alloy (denoted as 'Ca-free Mg alloy') prepared by the similar casting method was also purchased from the supplier. The chemical compositions of the alloys are listed in Table 1. These Mg alloys were pre-annealed at 683 K for 24 hours at the supplier. The cylindrical specimens (10 mm in diameter and 12 mm in height) for the forging were machined from the center of the billets. Upset forging was carried out by compressing the specimens to $\varepsilon = 1.6$ at 573 K with the true strain rate of $1.0 \times 10^{-1}\,s^{-1}$.

Table 1 Chemical compositions of Mg-Ca and Ca-free Mg alloys (in mass%).

	Al	Zn	Mn	Si	Fe	Cu	Ni	Ca	Mg
Mg-Ca	8.9	0.84	0.18	0.005	0.003	<0.002	<0.002	0.94	Balance
Ca-free	8.7	0.81	0.21	0.007	0.004	<0.002	0.002	0.002	Balance

The tensile specimens with 6 mm in gauge length and $1.6 \times 1.6\,mm^2$ in gauge width were cut from the unforged and forged Mg alloys. Tension tests were carried out at ambient temperature and 573 K with $1 \times 10^{-3}\,s^{-1}$. As for the forged specimens, the tensile direction was perpendicular to the forging direction. Microstructure of the specimens before and after tensile tests was investigated using an optical microscope. The grain size were measured by the line intercept method ($d = 1.74L$, where d and L are the grain size and the line intercept length, respectively).

3. Results

Microstructures of the unforged Mg-Ca alloy and Ca-free Mg alloy are shown in Fig. 1. Second phases were connected continuously for the Mg-Ca alloy. Preliminary elemental analyses suggested that the second phases were mainly Al_2Ca. The average grain size was 280 μm for the unforged Mg-Ca alloy and 150 μm for the unforged Ca-free Mg alloy.

Microstructures of the forged Mg-Ca alloy and Ca-free Mg alloy are shown in Fig. 2. The average grain size was 4.9 μm for the forged Mg-Ca alloy and 3.5 μm for the forged Ca-free Mg alloy. Grain refinement by the forging was obtained for both the Mg-Ca alloy and the Ca-free Mg alloy. In the forged Mg-Ca alloy, the second phases tended to be distributed

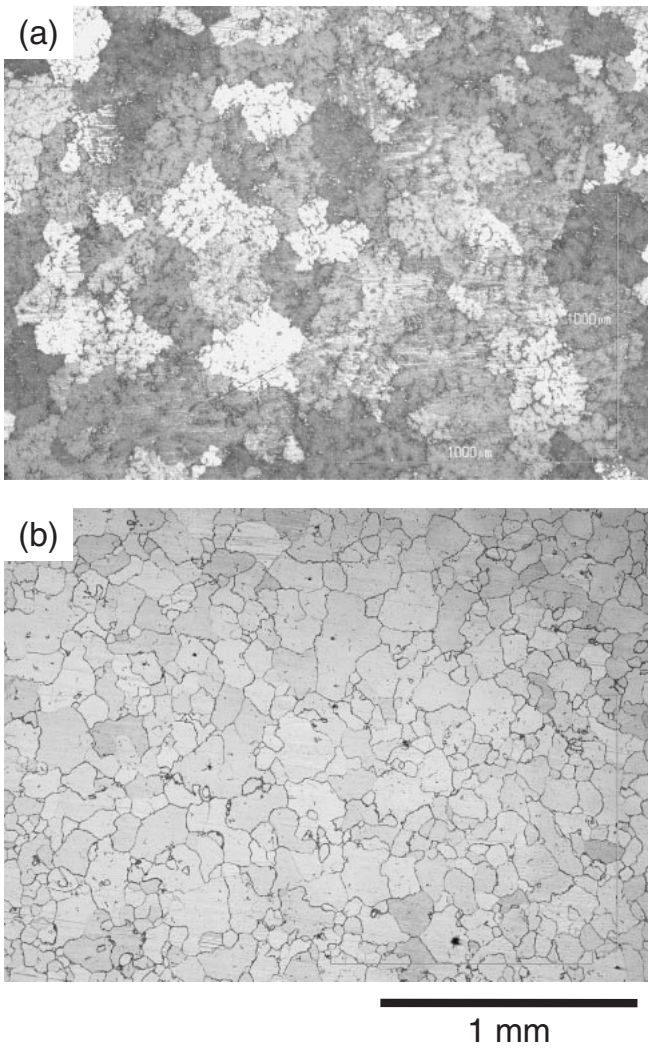

Fig. 1 Microstructures of unforged Mg alloys. (a) Mg-Ca and (b) Ca-free Mg alloys.

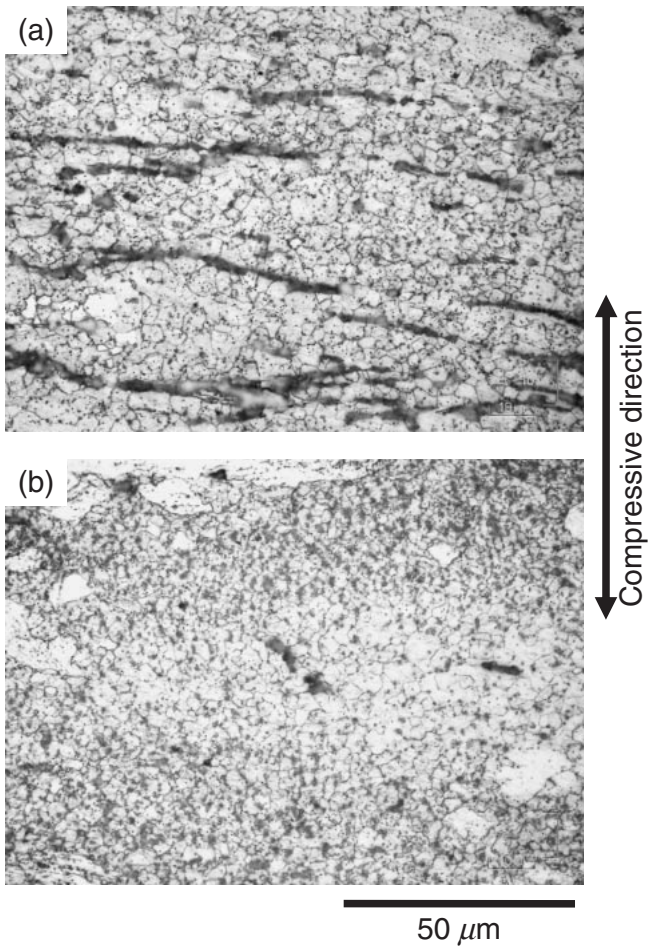

Fig. 2 Microstructure of forged Mg alloys. (a) Mg-Ca and (b) Ca-free Mg alloys.

perpendicularly to the compressive direction. The volume fraction of the second phases was approximately 2.5% in the Mg-Ca alloy, which was measured by the image analyses.

Enlargement of microstructure in the forged Mg-Ca and Ca-free Mg alloy is shown in Fig. 3. The second phases were not connected continuously, but were distributed as particles with an average diameter of 1.2 μm. Thus, the continuously-connected second phases were segmented during the upset forging. The second phase particles were located at grain boundaries.

The nominal tensile stress-strain curves of the unforged and forged specimen are shown in Fig. 4 for the Mg-Ca alloy and in Fig. 5 for the Ca-free Mg alloy, respectively. The testing temperature was ambient. Note that the tensile strength and elongation to failure were enhanced by hot forging for both the Mg-Ca alloy and the Ca-free Mg alloy. The enhancement of strength for the forged Mg alloys is mainly attributed to grain refinement by hot forging. The strengthening related to the second phases will be discussed later.

Summary of the tension tests at ambient temperature on the unforged and forged Mg alloys is shown in Table 2. It is found from the results of the unforged specimens that the Ca addition increased the 0.2% proof stress, but significantly reduced the elongation to failure. On the other hand, the 0.2% proof stress and ultimate tensile strength were increased by the forging, and furthermore, the decrease in elongation to failure caused by the Ca addition was reduced for the forged specimens, compared to the unforged specimens. This is likely to be attributed to segmentation of the second phases by the forging.

The nominal tensile stress-strain curves at 573 K for the unforged and forged Mg-Ca alloy are shown in Fig. 6. A large elongation to failure of 284% was obtained for the forged specimen, while that for the annealed specimen was 50%.

The forged Mg-Ca alloy specimen deformed to failure at 573 K is shown in Fig. 7. Broad necking, which is one of features in superplastic deformation, was observed. The superplastic-like deformation in the forged specimen is attributed to a small grain size of 4.9 μm. Occurrence of a large elongation of 284% in the Mg-Ca alloy indicates that good workability can be obtained in the forged Mg-Ca alloy due to grain refinement.

4. Discussion

The forged specimen showed much higher strength than the unforged specimen for both the Mg-Ca alloy and the Ca-

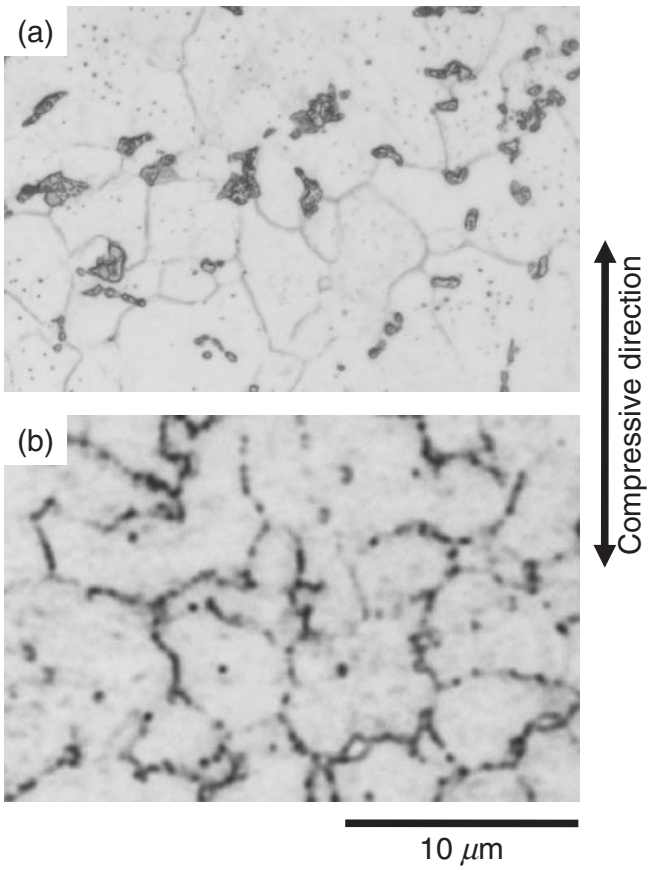

Fig. 3 Enlargement of Microstructures of forged Mg alloys. (a) Mg-Ca and (b) Ca-free Mg alloys.

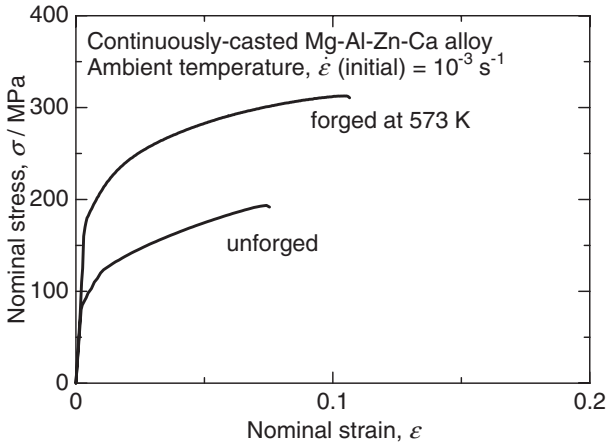

Fig. 4 Nominal stress-strain curves at ambient temperature for unforged and forged Mg-Ca alloy specimens.

free Mg alloy. This is attributed to grain refinement by the forging. Another important result is that the Mg-Ca alloy showed higher 0.2% proof stress than the Ca-free Mg alloy. This cannot be explained by grain refinement because the grain size of the Mg-Ca alloy was larger than that of the Ca-free Mg alloy.

A difference in 0.2% proof stress due to the grain refinement strengthening mechanism, $\Delta\sigma_{GS}$, can be estimated using the Hall-Petch equation of the form[13)]

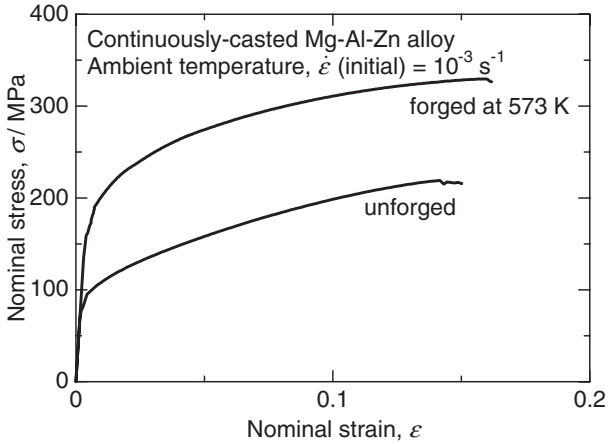

Fig. 5 Nominal stress-strain curves at ambient temperature for unforged and forged Ca-free Mg alloy specimens.

Table 2 Results of tension tests at ambient temperature on unforged and forged Mg-Ca and Ca-free Mg alloys.

	0.2% Proof stress (MPa)	Ultimate tensile strength (MPa)	Elongation (%)
Unforged			
Mg-Ca alloy	93	195	7.4
Ca-free Mg alloy	77	226	14.5
Forged			
Mg-Ca alloy	174	313	10.7
Ca-free Mg alloy	159	330	16.1

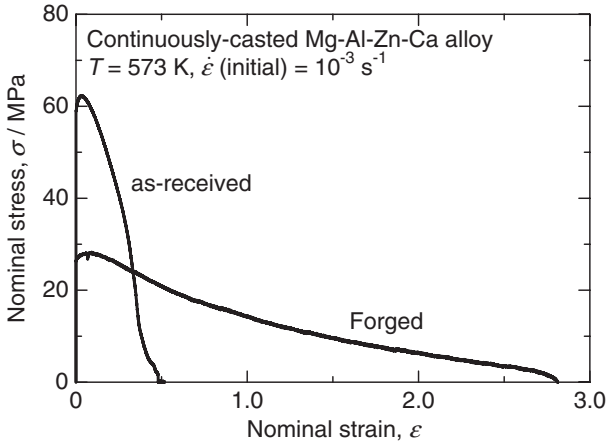

Fig. 6 Nominal stress-strain curves at 573 K for unforged and forged Mg-Ca alloy specimens.

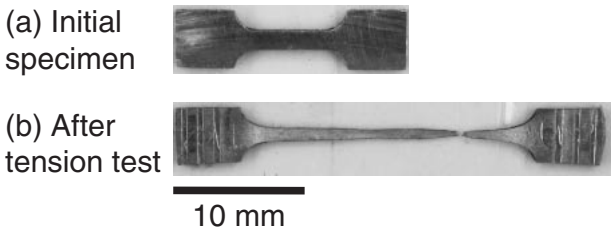

Fig. 7 Forged Mg-Ca alloy specimens (a) before and (b) after tension test at 573 K, showing a large elongation of 284%.

$$\Delta\sigma_{GS} = K(d_1^{-1/2} - d_2^{-1/2}), \quad (1)$$

where K is a constant (= 210 MN μm$^{-1/2}$ for Mg),[14] d_1 and d_2 are the grain size of materials 1 and 2. From eq. (1), $\Delta\sigma_{GS}$ between the forged Mg-Ca and Ca-free Mg alloys is calculated to be 17 MPa. Hence, an increase in 0.2% proof stress due the Ca addition is 32 MPa for the forged specimens, considering the difference in 0.2% proof stress between the forged Mg-Ca and Ca-free Mg alloys.

The interface between the Mg matrix and second phase in the Mg-Ca alloy is unlikely to be at a coherent state since lattice constants and crystal structures are different from each other. Therefore, strengthening mechanisms for metal matrix composites can be applied to the Mg-Ca alloy.[15] The Orowan mechanism is one of the strengthening mechanisms for metal matrix composites.[16] An increase in yield stress due to the Orowan mechanism, $\Delta\sigma_{Orowan}$, may be given by[16]

$$\Delta\sigma_{Orowan} = \frac{0.81MGb\ln(d_p/b)}{2\pi(1-\nu)^{1/2}(\lambda - d_p)}, \quad (2)$$

where M is the Taylor factor (= 6.5 for Mg),[13] G is the shear modulus of a matrix (= 1.66×10^4 MPa for Mg),[17] b is the Burgers vector of a matrix (= 3.21×10^{-10} m for Mg),[17] d_p is the mean particle size, ν is the Poisson's ratio and λ is the mean center-to-center spacing between particles (= $1/2d_p(3\pi/2f_v)^{1/2}$, where f_v is the volume fraction of the second phase). From eq. (2), $\Delta\sigma_{Orowan}$ due to the Ca addition is estimated to be about 6 MPa for the forged Mg-Ca alloy. Therefore, effect of the Orowan mechanism is minor in the Mg-Ca alloy.

The load transfer mechanism is also one of important strengthening mechanisms. From a shear lag mode, an increase in yield stress due to the load transfer mechanism, $\Delta\sigma_{LT}$, may be given by[16,18]

$$\Delta\sigma_{LT} = f_v\sigma_m/2 \quad (3)$$

where σ_m is the yield stress of a matrix. From eq. (3), $\Delta\sigma_{LT}$ due to the Ca addition is estimated to be 1 MPa for the forged Mg-Ca alloy. Therefore, the load transfer mechanism is not important in the Mg-Ca alloy.

Third strengthening mechanism is related to a difference in thermal expansion, namely, high dislocation density generated by a difference in thermal expansion between two components causes an increase in yield stress. An increase in yield stress due to a difference in thermal expansion, $\Delta\sigma_{CTE}$, may be given by[18,19]

$$\Delta\sigma_{CTE} = \alpha Gb\left(\frac{12\Delta T\Delta C f_v}{bd_p}\right)^{1/2}, \quad (4)$$

where α is a constant (= 1.25),[18] ΔT is the temperature change and ΔC is a difference in thermal expansion coefficients between a matrix (= 2.61×10^{-5} K^{-1} for Mg)[20] and a second phase particle. Unfortunately, a thermal expansion coefficient of Al_2Ca is unknown. Benci *et al.*[21] reported that that the thermal expansion coefficient of Al_2Ti is 1.2×10^{-5} K^{-1} at 473 K. Hence, assuming that a thermal expansion coefficient of Al_2Ca is the same as that of Al_2Ti, $\Delta\sigma_{CTE}$ due to the Ca addition is estimated to be 12 MPa for the forged Mg-Ca alloy.

Another possible strengthening mechanism is related to geometrical incompatibility between a matrix and a second phase. In this case, incompatibility between a matrix and a second phase particle causes generation of geometrically necessary dislocations during deformation, resulting in an increased strain hardening rate of a particle-reinforced metal, compared with a particle-free metal. An increase in yield stress due to the geometrical incompatibility, $\Delta\sigma_{geo}$, may be given by[18]

$$\Delta\sigma_{geo} = \alpha Gb\left(\frac{f_v 8\gamma}{bd_p}\right)^{1/2} \quad (5)$$

where γ is the shear strain calculated using the Taylor factor. From eq. (4), $\Delta\sigma_{geo}$ due to the Ca addition is estimated to be 17 MPa for the forged Mg-Ca alloy. Note that $\Delta\sigma_{Orowan} + \Delta\sigma_{LT} + \Delta\sigma_{CTE} + \Delta\sigma_{geo} = 36$ MPa is in agreement with an increase in 0.2% proof stress due the Ca addition for the forged Mg-Ca alloy (= 32 MPa), although the calculations contain considerable degree of assumption. Therefore, it is conclusively demonstrated that an increase in yield stress by the Ca addition is mainly due to the strengthening mechanisms related to a difference in thermal expansion and to geometrical incompatibility. As shown in eqs. (4) and (5), an increase in yield stress due to the strengthening mechanisms related to a difference in thermal expansion and to geometrical incompatibility is inversely proportional to the square root of the particle size. Therefore, it is required to obtain finer second phases for higher strength in the Mg-Ca alloy.

Usually, second phases are harmful to ductility and workability.[8] However, the forged Mg-Ca alloy showed a large elongation of 284% at 573 K, as shown in Fig. 5. At elevated temperatures, when stress concentration at a second particle is relaxed by diffusion, cavity formation is not enhanced by a second phase. Occurrence of stress concentration at the second phase can be estimated using the critical diffusion length parameter:[15,22,23] when the particle diameter is less than the critical diffusion length, the stress concentration due to the particle can be relaxed by diffusion and no cavities are formed. Because the second phases in the Mg-Ca alloy are located at grain boundaries, the critical diffusion length, Λ_{GB}, can be given by[22,23]

$$\Lambda_{GB} = \left(\frac{2.9\Omega\delta D_{GB}\sigma}{\phi dkT\dot{\varepsilon}}\right)^{1/2} \quad (6)$$

where Ω is the atomic volume, δ is the grain boundary thickness, D_{GB} is the grain boundary diffusion coefficient, σ is the stress, ϕ is the function of the total tensile strain accommodated by grain boundary sliding (= 0.6),[22] d is the grain size, k is the Boltzmann constant, T is the absolute temperature and $\dot{\varepsilon}$ is the strain rate. From eq. (6), Λ_{GB} under the test condition at 573 K is calculated to be 4 μm, which is larger than the average second phase particle diameter (= 1.2 μm) in the forged Mg-Ca alloy. Therefore, it is suggested that most second phases induce no stress concentration in the forged Mg-Ca alloy, resulting in a large elongation of 284%.

5. Conclusions

Mechanical properties of Mg-Al-Zn-Ca alloy (Mg-Ca

alloy) and Mg-Al-Zn alloy (Ca-free Mg alloy) were investigated by tension tests at ambient temperature and 573 K. The results are summarized as follows.

(1) The Mg-Ca alloy forged at 573 K showed the high 0.2% proof stress of 174 MPa. The high 0.2% proof stress is attributed not only to grain refinement by hot forging, but also to the strengthening mechanisms related to the thermal expansion coefficient difference and geometrical incompatibility between the Mg matrix and the second phases.
(2) The Ca addition decreased the elongation to failure, forming insoluble second phase particles. However, the decrease in elongation to failure by the Ca addition was reduced for the forged specimens, compared with the unforged specimens. This results from segmentation of the second phases by the forging.
(3) The forged Mg-Ca alloy showed a large elongation of 284% at 573 K because stress concentration at second phase particles could be relaxed by diffusion.

Acknowledgement

This study was conducted with the financial support by the "Forged Magnesium Parts Technological Development Project" which is organized by New Energy and Industrial Technology Development Organization (NEDO), Japan.

REFERENCES

1) T. Ebert and B. L. Mordike: Mater. Sci. Eng., A **302** (2001) 37–45.
2) R. Nimoniya, T. Ojiro and K. Kubota: Acta Metall. Mater. **43** (1995) 669–674.
3) A. A. Luo, M. P. Balogh and B. R. Powell: Metall. Mater. Trans. A **33A** (2002) 567–574.
4) Y. Chino, M. Kobata, H. Iwasaki and M. Mabuchi: Mater. Trans. **43** (2002) 2643–2646.
5) K. Ozturk, Y. Zhong, A. A. Luo and Z.-K. Liu: JOM **55** (2003) 40–44.
6) K. Hirai, H. Somekawa, Y. Takigawa and K. Higashi: Mater. Sci. Eng. A **403** (2005) 276–280.
7) S. Akiyama, H. Ueno, M. Sakamoto, H. Hirai and A. Kitahara: Materia Japan **39** (2000) 72–74.
8) R. Raj and M. F. Ashby: Acta Metall. **23** (1975) 653–666.
9) B. Jing, S. Yangshan, X. Feng, X. Shan, Q. Jing and T. Weijian: Scr. Mater. **55** (2006) 1163–1166.
10) H. Watanabe, M. Yamaguchi, Y. Takigawa and K. Higashi: Mater. Sci. Eng., A **454–455** (2007) 384–388.
11) Y. Chino, J. S. Lee, Y. Nakaura, K. Ohori and M. Mabuchi: Mater. Trans. **46** (2005) 2592–2595.
12) Y. Chino, Y. Nakaura, K. Ohori, A. Kamiya and M. Mabuchi: Mater. Sci. Eng. A **452** (2007) 31–36.
13) R. Armstrong, I. Codd, R. M. Douthwaite and N. J. Petch: Philos. Mag. **7** (1962) 45–58.
14) K. Kubota, M. Mabuchi and K. Higashi: J. Mater. Sci. **34** (1999) 2255–2262.
15) M. Mabuchi and K. Higashi: Acta Mater. **44** (1996) 4611–4618.
16) R. M. Aikin, Jr. and L. Christodoulou: Scr. Metall. Mater. **25** (1991) 9–14.
17) H. J. Frost and M. F. Ashby: *Deformation-Mechanism Maps*, (Pergamon Press, Oxford, 1982) p. 44.
18) J. W. Luster, M. Thumann and R. Baumann: Mater. Sci. Technol. **9** (1993) 853–862.
19) W. S. Miller and F. J. Humphreys: Scr. Metall. Mater. **25** (1991) 33–38.
20) *Kinzoku Data Book*, 3rd edn., (Maruzen, Tokyo, 1993) p. 14.
21) J. E. Benci, J. C. Ma and T. P. Feist: Mater. Sci. Eng. A **192–193** (1995) 38–44.
22) M. J. Stowell: Metal Sci. **17** (1983) 1–11.
23) K. T. Park, S. H. Myung, D. H. Shin and C. S. Lee: Mater. Sci. Eng. A **371** (2004) 178–186.